Catalysis Science & Technology

Accepted Manuscript

ROYAL SOCIETY OF CHEMISTRY

www.rsc.org/catalysis

Catalysis Science & Technology

ARTICLE

Dual resistance to alkali metals and SO_2: vanadium and cerium supported on sulfated zirconia as an efficient catalyst for NH_3-SCR

Received 00th January 20xx,
Accepted 00th January 20xx

DOI: 10.1039/x0xx00000x

www.rsc.org/

Shan Gao,[a,b] Penglu Wang,[a,b] Feixiang Yu,[a,b] Haiqiang Wang,[a, b*] Zhongbiao Wu,[a,b]

Vanadium and cerium supported on sulfated zirconia is an efficient SCR catalyst with dual resistance towards both potassium and SO_2 poisoning. To the best of our knowledge, no examples of catalysts with tolerance to both alkali metals and SO_2 have been reported. Catalyst having a Ce:V=1:1 molar ratio shows the highest activity (>97%) in the presence of potassium and SO_2. The formation of thermally stable $Ce_2(SO_4)_3$ disrupted the Ce(IV)/Ce(III) redox cycle, resulting in a significant deactivation of CeSZ catalyst (93% to 63% in 400 min). Vanadium additive led to the transformation of CeO_2 to $CeVO_4$, therefore cutoffs the reaction between CeO_2 and SO_2 and remains the reactivity of active sites. In addition, vanadium weakened the adsorption/oxidation of SO_2 on catalysts, and thus enhanced the tolerance toward SO_2 by inhibiting the formation of ammonium bisulfate (NH_4HSO_4).

1. Introduction

Selective catalytic reduction by ammonia (NH_3-SCR) is one of the efficient and mature technologies for abating NO_x emissions, and has been widely used throughout the world[1, 2]. V_2O_5-WO_3 (or MoO_3)/TiO_2 have been used as commercial catalysts for industrial applications during the last several decades. These catalysts are normally installed before electrostatic precipitator (ESP) and desulfurization[1], resulting in long time exposure to high concentrations of alkali metals and SO_2, which deactivates deNO_x catalysts and limits their lifetime[3-5].

Deactivation mechanism of alkali metals on catalysts are generally ascribed to the loss of surface acidity[3, 4, 6]. For vanadium based catalysts, alkali metals react with Brønsted acid sites (V-O-H), and inhibit the active sites (V^{5+}=O), which are both of importance for SCR reaction[4, 7]. Rasmus Fehrmann, et al[8-10] proposed high substrate acidity (sulfated, heteropoly acid promoted) is beneficial to increasing alkali resistance. Yue Peng, et al[11] also proposed that decreases in Brønsted acid sites that caused by alkali metals are responsible for deactivation of CeO_2-WO_3 catalyst.

Different effects of SO_2 have been discussed depending on the temperature range. For high temperature NH_3-SCR catalysts (300-450 °C), positive and negative effects of SO_2 have both been reported: Newly formed Brønsted acid would benefit the catalytic performance, while the formation of weakly reversibly sulfates would inhibit the activity[5, 12]. Besides, chemical transformation of active sites (e.g.: MnO_x, CeO_2) would occur to produce sulfate salts in the presence of SO_2 and H_2O, which is the main reason for catalytic deactivation[13, 14]. For CeO_2 catalyst, coupling with other metal oxides (such as Sn and Cu) is conductive to improving the resistance towards SO_2 and H_2O[15, 16].

Numerous efforts have been devoted to developing alkali metal-resistant or SO_2-resistant catalysts for SCR process. To our best knowledge, there has been little reports about catalysts with tolerance to both alkali metal and SO_2. Our recent preliminary papers[17-19] has reported that ceria supported on sulfated zirconia shows enhanced resistance towards alkali metal , when the superacid sites could preferentially react with alkali metals and retard the decrease of acidity. In the present study, we investigated the effects of SO_2 on as-prepared catalyst, and improve its SO_2 resistance by vanadium additive.

2. Materials and methods

2.1 Catalyst preparation

All the catalysts were prepared via consecutive impregnation methods according to our previous study[17-19]. Cerium(III) nitrate hexahydrate and/or ammonium metavanadate are used as catalyst precursors, and were dissolved in deionized water and oxalic acid solution, respectively. Cerium catalyst supported on sulfated zirconia is referred to as CeSZ, vanadium catalyst supported on sulfated zirconia is denoted as

[a] Key Laboratory of Environment Remediation and Ecological Health, Ministry of Education, College of Environmental & Resources Science, Zhejiang University, 310058 Hangzhou, P.R. China; Fax: +86 571 8795 3088; Tel: +86 571 8795 3088; E-mail: haiqiangwang@zju.edu.cn.
[b] Zhejiang Provincial Engineering Research Center of Industrial Boiler & Furnace Flue Gas Pollution Control, Hangzhou 310027, P.R. China.
†Electronic Supplementary Information (ESI) available. See DOI: 10.1039/x0xx00000x

VSZ. Cerium and vanadium supported on sulfated zirconia are designated as CeVSZ(x), where x is indicative of V/Ce molar ratios. The designed mole ratio of Me (Me = Ce + V) to Zr is 0.095. K-poisoned catalysts are designated as KCeSZ, KCeVSZ, or VSZ, and K/Me mole ratio is 0.4.

2.2 SCR activity evaluation

Selective catalytic reduction of NO with NH_3 was carried out in a fixed-bed quartz reactor (1 cm i.d.) by using 0.5 g catalyst of 40-60 mesh. Typical composition of inlet gas was 600 ppm NO, 600 ppm NH_3, 3.5 % O_2, 5 % H_2O (when used), 600 ppm SO_2 (when used) and balanced with N_2. The gas hourly space velocity (GHSV) was kept at around 180,000 h^{-1}. The concentrations of NO, NO_2, and O_2 were monitored by a flue gas analyzer (Testo 350, Testo Inc., Germany). N_2O was detected by an FT-IR gas analyzer (Madur Photon Portable IR Gas Analyzers, Madur Ltd., Austria).

2.3 Characterizations

The crystal phases of the samples were identified by using X-ray diffraction (XRD) with Cu Kα radiation (model D/max RA, Rigaku Co., Japan). The scanning range (2θ) was collected from 10 and 80° with a step size of 0.02°. The specific surface areas were determined by the Brunauer-Emmett-Teller (BET) method on a nitrogen adsorption apparatus (ASAP 2020, USA). All the samples were degassed at 300°C prior to measurements. The data were collected in the relative pressure (P/P_0) ranging from 0.05 to 0.30. The Raman spectra of samples were collected at a Raman Spectrometer (Raman: Jobin-Yvon LabRAM HR800), using a laser at 514.5 nm line as the excitation source. The laser power of the 514.5 nm line at the samples was below 1.0 mw. X-ray photoelectron spectroscopy (XPS: Thermo ESCALAB 250, USA) was used to investigate the surface properties of the samples, with Al Kα radiation (hv = 1486.6 eV). The shift of the binding energy due to relative surface charging was corrected using the C 1s level at 284.8 eV as an internal standard. In situ DRIFTS experiments were carried out by using Nicolet 6700 FTIR spectrometers. Catalyst was pre-treated at 450 °C under He (30 mL/min) for 60 min to remove adsorbed impurities. The background spectrum was recorded in flowing He and was subtracted from catalyst spectra. DRIFTS spectra of samples were recorded at 350 °C by accumulating 32 scans with a resolution of 4 cm^{-1}.

3. Results and discussion

3.1 Catalytic activity

The effects of SO_2 on the SCR activity of NO by NH_3 over CeSZ, CeVSZ, and VSZ catalysts were monitored as a function of time at 350 °C (Fig. 1). Before exposing catalysts to SO_2, the NO conversions of all the catalysts were over 90%, and the initial SCR activity at 350 °C decreased in the following sequence: VSZ = CeVSZ(2) > CeVSZ(1) > CeVSZ(0.5) > CeSZ. After 600 ppm SO_2 was introduced to the steam, the catalytic activity of CeSZ catalyst declined significantly from 93% to 63% in 400 min. When ceria was partially replaced by vanadia, the decrease NO conversion became less obvious upon the addition of SO_2. When V/Ce mole ratio value was over 1:1, the catalytic performance seems stable in 400 min and to be unaffected by SO_2. CeVSZ(2) and VSZ catalysts maintained 100% of NO conversion at 350 °C with no tendency to decrease in 400 min.

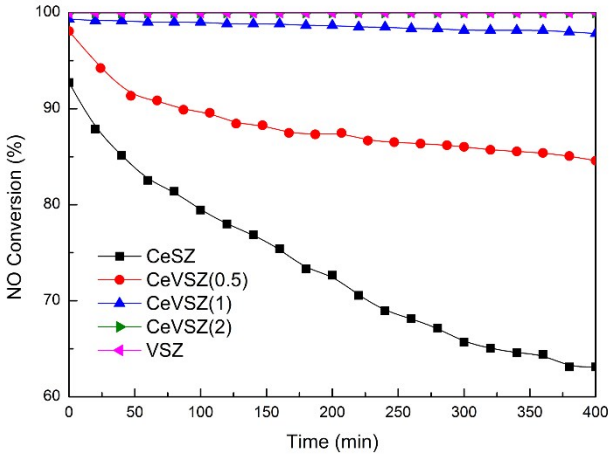

Fig. 1. The effect of SO_2 on NO conversion for CeSZ, CeVSZ, and VSZ catalysts.

The performance of K doped catalysts was also tested in the presence of SO_2 (shown in Fig. 2). Similar with CeSZ, KCeSZ catalyst displays a gradual deactivation by SO_2 exposure. NO conversion of KCeSZ dropped from 95% to 64% in 400 min. In contrast, K doped VSZ catalyst obtains only 75% NO conversion before SO_2 was added into the stream, showing a low tolerance towards potassium in spite of a strong resistance to SO_2. Regardless of the V/Ce ratios, all the K doped CeVSZ catalysts present superior SCR performance and enhanced SO_2 resistance, when their NO conversions remain over 95% within 400 min after SO_2 was introduced into the stream. Among these co-supported catalysts, CeVSZ(1) exhibited the highest activity (> 97%) during the whole test time.

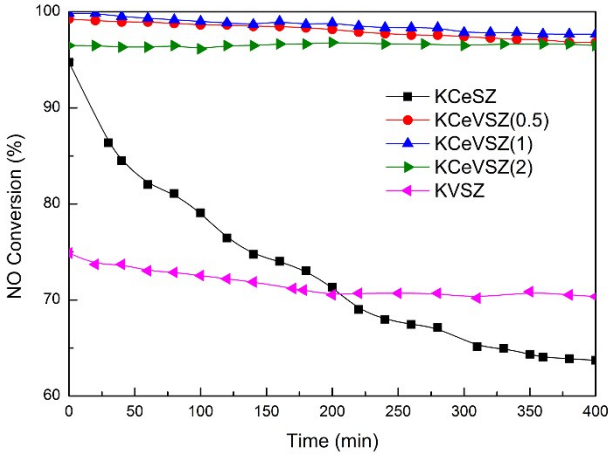

Fig. 2. The effect of SO_2 on NO conversion for KCeSZ, KCeVSZ, and KVSZ catalysts.

To further investigate the alkali resistance of CeVSZ(1) catalyst, various K amounts were added onto the catalyst, and their activities in the presence of SO_2 were tested (showed in Fig. S1). All the catalysts with various K amounts show stable NO conversions within 400 min, and SO_2 has no deactivation effects on their catalytic performance. With increasing amount

of K, the catalytic activity of catalyst decreases accordingly. When compared with V_2O_5-WO_3/TiO_2 catalyst (commercial catalyst), CeVSZ(1) catalyst shows much stronger potassium resistance. It has been reported[17] that a small amount of K (1.0 wt.%) resulted in a complete deactivation of V_2O_5-WO_3/TiO_2 catalyst (< 20%). In contrast, CeVSZ(1) catalyst with 1.2 wt.% K still possesses over 97% NO conversion. Only when K amount increased to 4.8%, did CeVSZ(1) catalyst become significantly deactivated (ca. 10%).

Except for alkali metals and SO_2, the deactivation effects of H_2O on SCR catalysts are also a matter of concern in potential practical applications. Therefore the catalytic performance of catalysts were tested when poisoned by potassium, SO_2, and H_2O simultaneously (Fig. S1). In the presence of 1% K, 600 ppm SO_2, and 5% H_2O, CeVSZ(1) still shows a stable activity (>95%) within 400 min at 350 °C, revealing the excellent resistance in potential practical applications. Although SO_2 and H_2O has negligible effects on the performance of V based catalysts, K could significantly deactivate VSZ, resulting in a notable decrease in the activity of VSZ (from 100% to 70%). For CeSZ, its activity was basically unaffected by potassium. However, 600 ppm SO_2 and 5% H_2O caused a distinct deactivation of KCeSZ catalyst from 97% to 53% in 400 min. When comparing catalysts in SO_2 and H_2O with that in SO_2, H_2O in the stream has negligible effects on the NO conversion of catalysts.

To clarify the nature of the effects of SO_2 on the different catalysts, and to explain the enhanced SO_2 resistance of Ce and V co-doped catalysts, various characterizations of the catalysts were conducted. Fresh and SO_2 poisoned catalysts were also investigated in present paper.

3.2 Crystallization

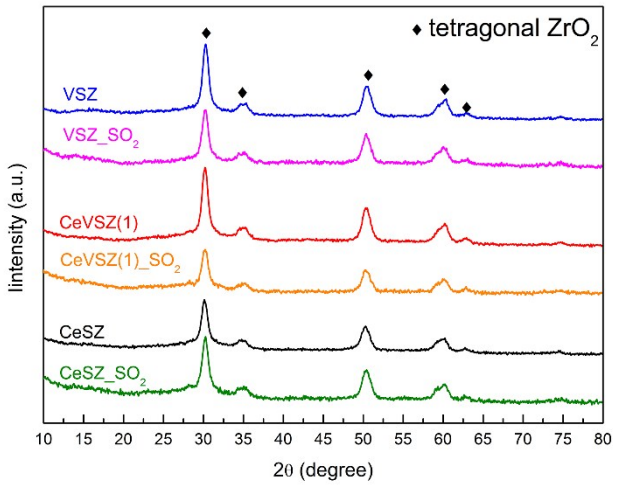

Fig. 3. XRD patterns of fresh and SO_2 poisoned catalysts.

The powder X-ray diffraction patterns of the fresh and SO_2 poisoned catalysts are depicted in Fig. 3. All the catalysts supported on sulfated zirconia presents typical diffraction patterns of tetragonal zirconia (PDF-ICDD 50-1089: 2θ = 30.3°, 35.3°, 50.4°, 60.2°, 63.0°). No distinct peaks corresponding to cerium or vanadium species could be detected in the patterns of these catalysts, indicating that active components are well dispersed on zirconia supports. After catalysts were poisoned by SO_2 for 400 min, no new peaks emerged, and no obvious changes in peak positions were observed. It suggested that no crystalline bulk sulfates formed on the surface of catalyst (which may be in the amorphous state)[14].

3.3 Surface area

Table 1: Surface area of fresh and SO_2 poisoned catalysts.

	K-free (m^2/g)	K-dope (m^2/g)
CeSZ	44.2	68.5
CeSZ_ SO_2	38.5	60.2
CeVSZ (1)	37.6	60.3
CeVSZ (1)_ SO_2	34.4	57.3
VSZ	59.6	45.2
VSZ_ SO_2	55.5	39.0

The BET surface areas of fresh and SO_2 poisoned catalysts are summarized in Table 1. As reported in our previous paper, the surface area of CeSZ catalyst increased from 44.2 m^2/g to 68.5 m^2/g after K introduction, indicated some textural modification effects caused by doped K[18]. Similar increase could also be observed in CeVSZ(1) catalyst (37.6 m^2/g to 60.3 m^2/g). But for VSZ catalyst, the surface area decreased from 59.6 m^2/g to 45.2 m^2/g after K poisoning.

The surface area of catalysts decreased by 3-8 m^2/g after the exposure of catalysts to SO_2 for 400 min. Among them, surface area of KCeSZ decreased most significantly. It was reported that the surface area is one of the dominant deactivation parameter for vanadia-alumina catalyst, when the deactivation behaviour was related with BET surface area as SO_2 deactivation progressed[20]. But for CeSZ and KCeSZ catalyst, their surface area only decreased by 5-8 m^2/g after reaction in SO_2, while their activities dropped ca 30%. Hence the surface area may not be the primary reason for decreased activity, and some other parameters should be responsible for the reduced activity.

3.4 Raman spectra

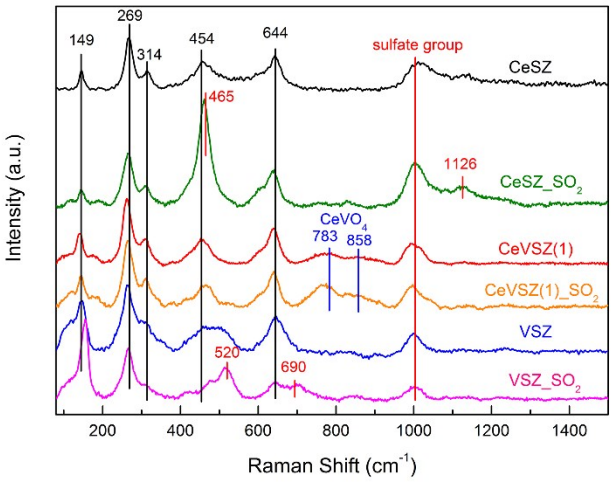

Fig. 4. Raman spectra of catalysts

The Raman spectra of catalysts were illustrated in Fig. 4. Bands at 149, 269, 314, 454, 644 cm^{-1} were detected for all the catalysts, which were attributable to the Raman-active modes

for the tetragonal phase of ZrO_2[21, 22]. A band at 1017 cm^{-1} was ascribed to the reflection of sulfate group[22]. It is worth nothing that two spectral bands were observed at 783, 858 cm^{-1} for CeVSZ(1) catalyst, which is typical characteristic of $CeVO_4$[23, 24]. The appearance of these two bands suggested the formation of $CeVO_4$ when vanadium was loaded on the ceria based catalysts.

Fig. 4 also presents the Raman spectra of catalysts after SO_2 exposure. A band at 465 cm^{-1} became apparent and was identified as symmetric O-Ce-O stretching mode of CeO_2[25]. In addition, a band emerged at 1126 cm^{-1}, corresponding to spectrum of $Ce_2(SO_4)_3$[26, 27]. This result implied that $Ce_2(SO_4)_3$ formed during the reaction of ceria catalyst with SO_2 in the presence of O_2. Furthermore, the formative $Ce_2(SO_4)_3$ were highly thermal stable and would decompose at about 840 °C[28]. The decomposition temperature may lower to 785 °C when ceria could act as a catalyst[27]. But in the temperature range of SCR reaction (300-500 °C), formed $Ce_2(SO_4)_3$ on the surface of CeSZ catalyst did not seem to decompose, resulting in the deactivation of active sites in the presence of SO_2. Similar result[14] has also been reported for CeO_2/TiO_2 catalyst in the reaction with SO_2, where high thermally stable $Ce(SO_4)_2$ and $Ce_2(SO_4)_3$ would disrupt the redox properties between Ce(IV) and Ce(III) and inhibit the formation and adsorption of nitrate.

In terms of CeVSZ(1) catalyst, no bands related to $Ce(SO_4)_2$ or $Ce_2(SO_4)_3$ were detected, indicating $CeVO_4$ species on CeVSZ(1) were unlikely to react with SO_2 to produce ceria sulfates. For the Raman spectra of VSZ catalyst, new bands appears at 520, 690 cm^{-1} after SO_2 exposure, which correlates well with $VO_2(SO_4)_2^{3-}$, $(VO)_2O(SO_4)_4^{4-}$, respectively[29]. These formed sulfates at/near the V sites has been reported to have promotion effects on the de-NO_x activity by increasing the surface acidity[30]. Besides, unlike thermally stable $Ce(SO_4)_2$, vanadyl sulfates and/or vanadium sulfate formed during the reaction would decompose below 400 °C[20]. This makes sure the regeneration of active site (V_2O_5), therefore catalyst can remain highly active without being deactivated by SO_2.

3.5 Surface elements

XPS was conducted to identify the surface nature and element concentrations of these catalysts. The surface concentrations of various elements are summarized in Table 2. After exposing catalysts to SO_2 for 400 min, a slight increase in N percentage was observed (binding energy at ca. 402 eV, spectra were not shown for the sake of brevity), which was an typical feature for an ammonium compound[31]. This may due to the formation and accumulation of NH_4HSO_4 and $(NH_4)_2SO_4$ on the surface of catalysts, which has been reported to cause a deactivation of the SCR catalysts[32-34].

The exposure of the fresh catalyst to SO_2 also resulted in an increase of surface S percentage, and the S $2p_{3/2}$ binding energies of these samples (ca. 169.5 eV, not shown, for the sake of brevity) were consistent with the S(VI) oxidation state[35, 36]. It was noteworthy that the increase of S concentration (by 1.17%) was much higher than that of N (by 0.63%) for CeSZ catalyst, while the increase of N and S were quite close for CeVSZ and VSZ catalysts (0.29% to 0.51%). This noticeable increase in S(VI) concentration revealed the formation of sulfate components ($Ce_2(SO_4)_3$) in addition to NH_4HSO_4 and $(NH_4)_2SO_4$, which was consistent with the result obtained by Raman spectra.

Table 2: XPS results for fresh and SO_2 poisoned catalysts.[1]

		S(%)	O_a(%)[2]	O_b(%)[3]	O_c(%)[4]	N(%)
CeSZ	Fresh	3.70	35.33	29.43	10.04	0.36
	SO_2 poisoned	4.87	29.11	34.47	10.02	0.99
CeVSZ(1)	Fresh	5.49	26.78	37.31	11.86	0.82
	SO_2 poisoned	5.78	25.21	38.67	11.15	1.32
VSZ	Fresh	5.03	27.30	38.06	10.89	1.23
	SO_2 poisoned	5.41	26.08	39.14	10.16	1.74

1. all the data were present in mole fraction for surface concentrations of various element
2. Oa (%): crystal lattice oxygen (ca. 530.0 eV)
3. Ob (%): hydroxyl species (ca. 531.8 eV)
4. Oc (%): chemisorbed water (ca. 533.3 eV)

The fitted O 1s spectra of catalysts before/after SO_2 exposure are shown in Fig. S2. Several species of oxygen existed on the surface of catalysts: crystal lattice oxygen O_a (ca. 530.0 eV), hydroxyl species and/or sulfates O_b (ca. 531.8 eV), and chemisorbed water O_c (ca. 533.3 eV)[37-39]. The calculated results are presented in Table 2, which shows SO_2 exposure resulted in an increase of O_b, especially for CeSZ catalyst. This result also validated the formation of surface sulfates (O_b[36, 40]) on CeSZ was more significant than that on CeVSZ and VSZ catalysts.

The representative photoelectron peaks of Ce 3d and V 2p pertaining to fresh and SO_2 exposed samples are depicted in Fig. 5. As one can see in Fig. 5a, peaks labelled u, u2, u3, v, v2, and v3 (in black) represent the $3d^{10}4f^0$ state of Ce(IV), while the peaks at labelled u1 and v1 (in red) represent the $3d^{10}4f^1$ initial electronic state corresponding to Ce(III)[38]. Ce (3d) spectra show that only Ce^{3+} ions existed on the surface of CeVSZ while both Ce^{4+} and Ce^{3+} ions exhibited on CeSZ catalyst. For CeSZ catalyst, the Ce^{3+} peaks (u1, v1) became more distinct after catalyst was exposed to SO_2, indicating a portion of Ce^{4+} ions transformed into Ce^{3+} ions in the presence of SO_2 and O_2. It has been reported that CeO_2 on Ce based catalysts could react with gaseous SO_2 according to the following reaction[14, 41, 42]: $2CeO_2 + 3SO_2 + O_2 \rightarrow Ce_2(SO_4)_3$. This reaction could take place at a lower temperature in the presence of O_2 (< 300 °C) with a high yield[41]. And this result agrees well with Raman spectra and the discussion above.

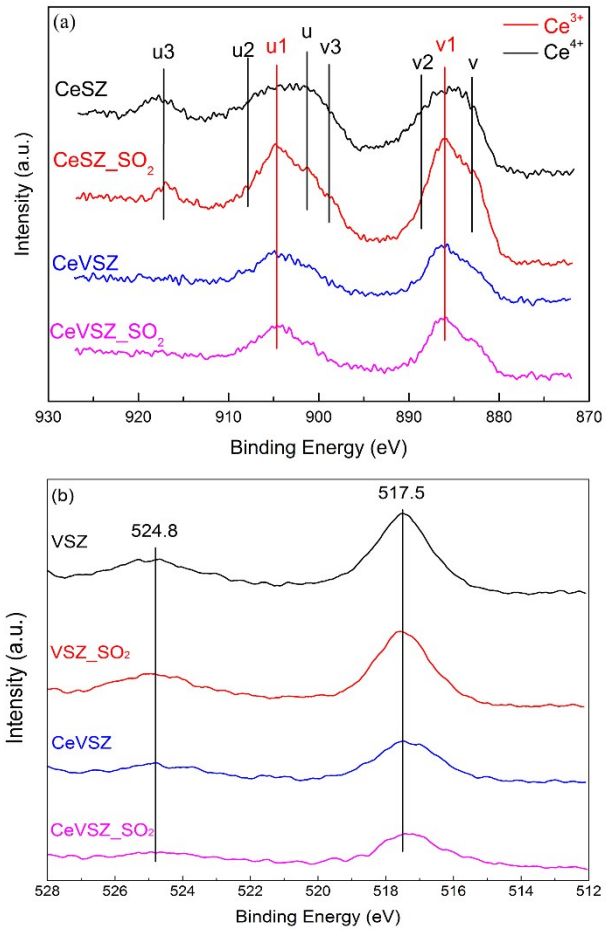

Fig. 5. XPS spectra of (a) Ce 3d and (b) V 2p.

By contrast, the only observable peaks in Ce 3d spectra of CeVSZ(1) were addressed to the $3d^{10}4f^{1}$ initial electronic state of Ce(III). The absence of peaks at u3 is direct evidence that Ce on the surface of CeVSZ(1) was in the Ce(III) state, confirming the formation of $CeVO_4$ and a negligible amount of CeO_2. CeO_2 is highly active for SCR reaction, but it would easily react with SO_2 in the presence of O_2, resulting in the deactivation of active sites[14]. When ceria was partially replaced by vanadia on sulfated zirconia (Ce/V = 1:1), all supported ceria transformed into $CeVO_4$ on the surface of catalysts. $CeVO_4$ is also considered as an active catalyst for SCR reaction. It has been reported $CeVO_4$ exhibit relatively low energy barriers and high SCR activity, and could also be served as the Brønsted acid sites[43]. Exposure of CeVSZ(1) catalyst to SO_2 caused no notable change in XPS spectra of Ce 3d, suggesting that SO_2 would not react with $CeVO_4$ and has neglectable influence on Ce state.

Furthermore, the spectra of V 2p is also depicted in Fig. 5b. The peaks at binding energies of 524.8 (V $2p_{1/2}$) and 517.5 eV (V $2p_{3/2}$) are a split signal of V 2p, which were assignable to the surface V^{5+} species[44-46], implying vanadium ions in CeVSZ and VSZ catalysts are mostly presented as V^{5+}. Spectra of catalyst are similar before or after SO_2 poisoning, indicating the introduced SO_2 does not influence the valence states of vanadium components.

3.6 In situ DRIFT

The SO_2 adsorption and reaction on catalysts was studied by the use of in situ DRIFT spectroscopy.

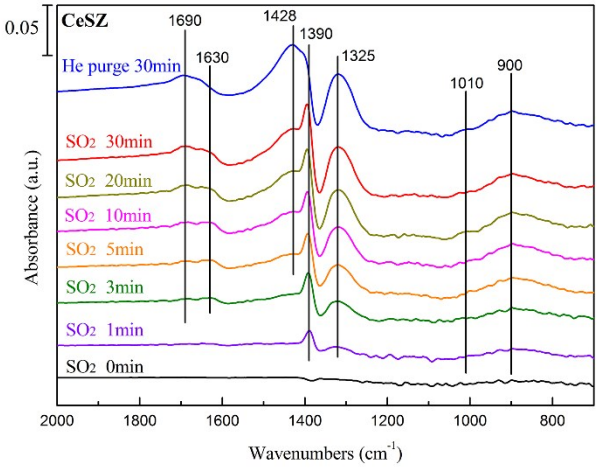

Fig. 6. DRIFT spectra of CeSZ catalyst exposed to 600 ppm SO_2/He + 3% O_2/He at 350 °C.

Fig. 6 shows the spectra collected at different time intervals when CeSZ catalyst was exposed to 600 ppm SO_2 and 3% O_2. Several bands at 1690, 1630, 1428, 1390, 1325, 1010, and 900 cm^{-1} were detected. The bands at 1690, and 1630 cm^{-1} could be attributed to the deformation mode of H_2O[14, 47, 48], which indicates the formation of water molecule as a reaction product after SO_2 adsorption (which will be discussed later). A weak band emerged at ca. 1428 cm^{-1} was reported to be related to the formation of SO_3 species[12]. One broad band at ca. 1390 cm^{-1} characterizes the formation of surface sulfate species with only one S=O bond, the species being bonded to the surface by the other three oxygen atoms[49, 50]. In addition, the band centred at 1325 cm^{-1} has been interpreted as an asymmetric stretch of physisorbed SO_2[51].

Fig. 6 also shows a broad band between 800 and 1050 cm^{-1}, with features at 900 and 1010 cm^{-1}, which were assigned to surface sulfite[52]. It has been reported[51, 52] that SO_2 could react with hydroxyl groups on oxide particles according to the following equation:

$$2OH^{-}(a) + SO_2 \rightarrow SO_3^{2-}(a) + H_2O \quad (1)$$

The consumption of surface OH species at 3730, 3660 cm^{-1} (shown in Fig. S4) also indicates the reaction between SO_2 and surface OH could occur.

When the sample was flushed with He steam for 30 min, the band at 1390 cm^{-1} gradually decreased, while that at 1428 cm^{-1} enhanced simultaneously. This may caused by the decomposition of unstable tridentate surface sulfates to SO_3 species.

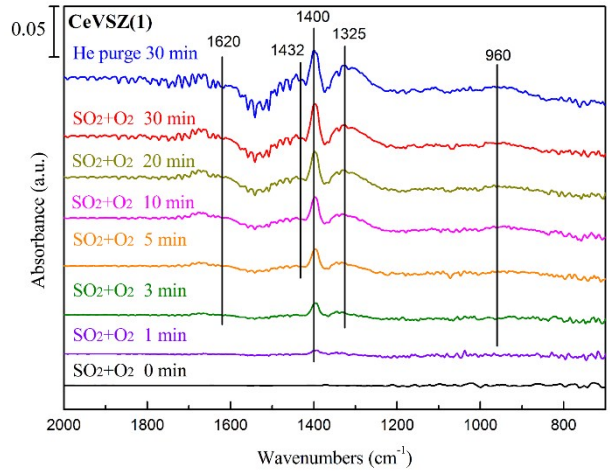

Fig. 7. DRIFT spectra of CeVSZ(1) catalyst exposed to 600 ppm SO_2/He + 3% O_2/He at 350 °C.

Fig. 7 shows the DRIFT spectra when CeVSZ(1) catalyst was purged by 600 ppm SO_2 and 3% O_2 for 30 min at 350 °C. Two peaks at ca. 1400 and 1325 cm^{-1} and two shoulders around 1620, and 1432 cm^{-1} were detected, which were attributed to tridentate sulfates[49, 50], physisorbed SO_2[51], H_2O molecule[14, 47], and SO_3 species[12], respectively. A weak band around 960 cm^{-1} was assigned to surface sulfite[52]. CeVSZ(1) catalyst showed similar spectra with CeSZ, but with much lower intensity, indicating weaken ability for adsorbing SO_2 and for oxidizing SO_2 to SO_3, sulfites, and sulfates.

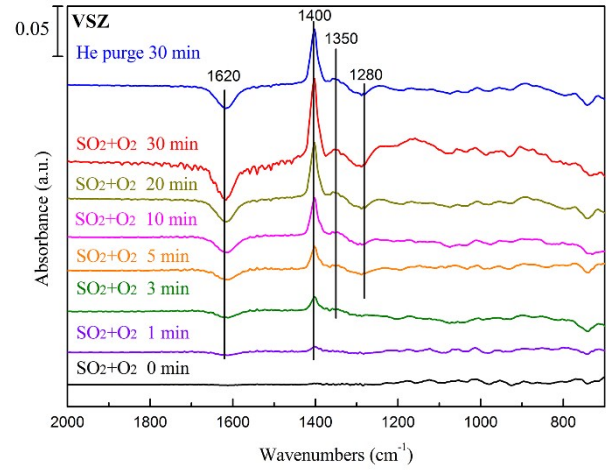

Fig. 8. DRIFT spectra of VSZ catalyst exposed to 600 ppm SO_2/He + 3% O_2/He at 350 °C.

VSZ catalyst was also exposed to 600 ppm SO_2 and 3% O_2, as shown in Fig. 8. A strong band was detected at 1400 cm^{-1}, which was due to tridentate sulfates[49, 50] (similar with CeVSZ(1) and CeSZ). A weak shoulder at ca. 1350 cm^{-1} was attributed to the v_3 vibrational mode of gaseous SO_2[53]. It is noted that no band related to SO_3 (1428 cm^{-1}) or physisorbed SO_2 (1325 cm^{-1}) was detected in terms of VSZ. This result suggested the adsorption and oxidation of SO_2 on VSZ was relatively weaker, leading to an enhanced tolerance towards SO_2. Additional, two negative bands were observed, a moderate band at ca. 1620 cm^{-1}, and a weak one around 1280 cm^{-1}. These two bands might be ascribed to surface oxalate complexes[54-57], which was introduced from oxalic acid during catalyst preparation (as cosolvent) and consumed in SO_2 purging process (possibly react with SO_3 or/and other oxidative components).

Several points that should be stressed from the discussion of in situ DRIFT were: (1) Considerable adsorption and oxidation reaction of SO_2 would occur on the surface of CeSZ catalyst, resulting in the formation of SO_3 and sulfates, which explains the poor tolerance to SO_2; (2) The introduction of V into the catalyst weakens the SO_2 adsorption and oxidation on the catalyst, therefore improve the SO_2 resistance.

3.7 Surface acidity

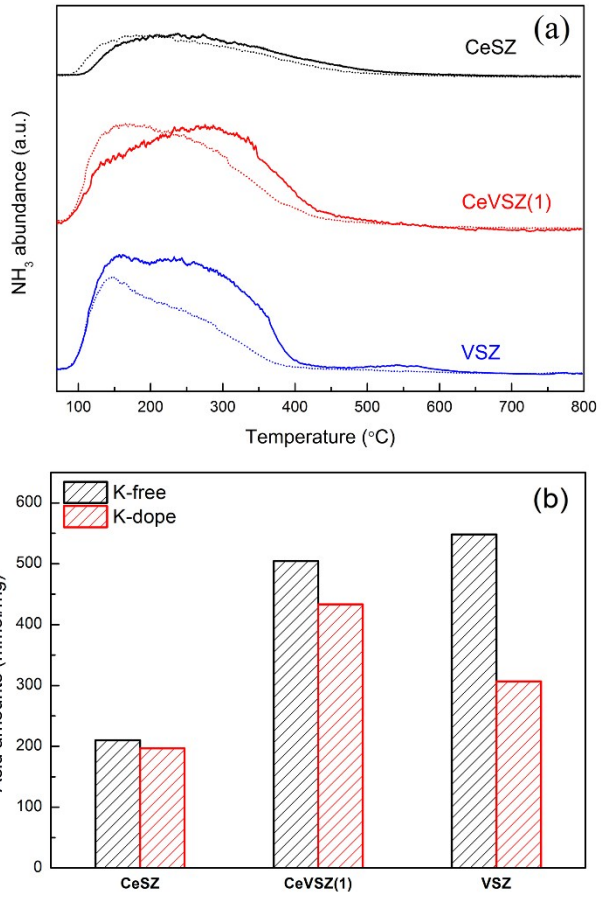

Fig. 9. (a) NH_3-TPD profiles of catalysts. Solid line for fresh samples, dash line for K-poisoned ones. (b) Acid amounts of K-free and K-doped catalysts.

NH_3-TPD experiments were performed over fresh and K poisoned catalysts, and the desorbed ammonia was detected by a mass spectrometer (profiles shown in Fig. 9a, Solid line for fresh samples, and dash line for K-poisoned ones). The acid amounts of different catalysts were calculated and shown in Fig. 9b. The acid amounts of V-containing catalysts are considerably larger than that of CeSZ catalyst (more than two times). Most of the adsorbed NH_3 desorbed below 500 °C. The addition of K significantly decreased the acid amount of VSZ, especially during 150-400 °C. For CeSZ and CeVSZ catalysts, the majority of their acid amounts remains after K doping. The NH_3

desorption peaks shifted to lower temperature for CeSZ and CeVSZ catalysts, indicating strong acid sites transformed to weaker ones. Our previous work[17] has proposed that small amount of potassium could alter some Brønsted acid sites to Lewis ones, therefore retaining the majority of acid amount. And this transformation of acid types may influence the catalyst ability to adsorb NH_3. Catalyst acidity is responsible for adsorbing NH_3, which facilitate SCR reaction[58, 59]. Therefore adequate surface acidity is necessary for high activity in SCR reaction.

DRIFTS experiments of NH_3 adsorption were conducted to investigate the acid types and quantities. Fig. 10a, and b show spectra of adsorbed NH_3 species on fresh, and K-poisoned CeSZ, CeVSZ(1), and VSZ catalysts in flowing NH_3/He at 350 °C and then purged by He for 30 min.

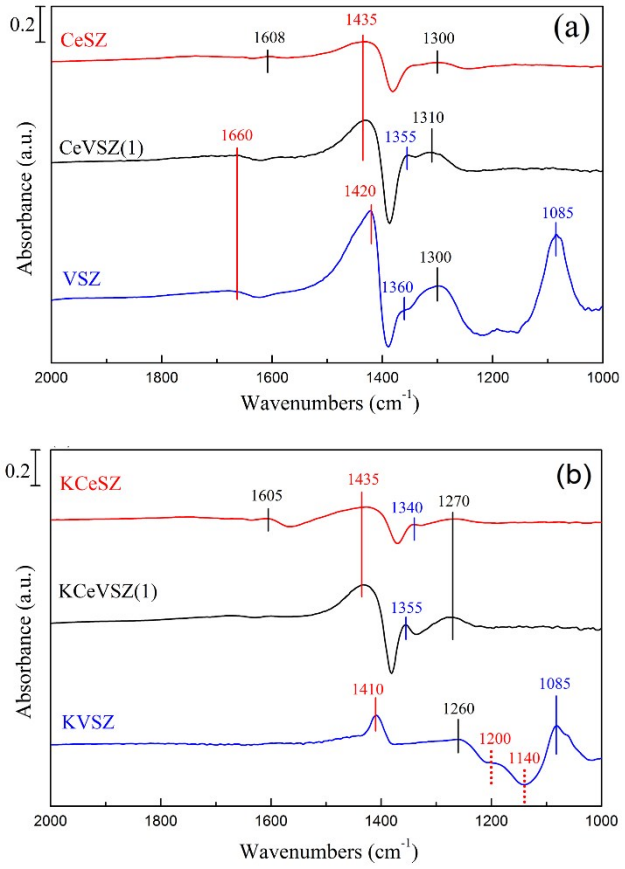

Fig. 10. DRIFT spectra of (a) fresh catalysts, and (b) K-poisoned catalysts exposed to 1000 ppm NH_3/He at 350 °C.

When NH_3 was adsorbed onto CeSZ catalyst (Fig. 10a), two weak bands at ca. 1608, and 1300 cm^{-1} were assigned to NH_3 coordinated at Lewis acid sites[60-62], while one strong band at around 1435 cm^{-1} was attributed to asymmetric bending vibrations of NH_4^+ on Brønsted acid sites[63, 64]. The spectra of KCeSZ catalyst (Fig. 10b) shared a similar pattern with CeSZ, additional a new band at 1340 cm^{-1} was assigned to -NH_2 wagging[65].

When NH_3 was adsorbed onto VSZ catalyst (Fig. 10a), several bands at 1660、1420、1360、1300、1085 cm^{-1} were detected. A strong band at 1420 cm^{-1} and a weak one at 1660 cm^{-1} were due to NH_4^+ species on Brønsted acid sites[64], and the band at 1300 cm^{-1} was ascribed to NH_3 coordinated at Lewis acid sites[60-62]. A small shoulder near 1360 cm^{-1} does not belong to hydroxylamine-like adsorbed species, and several authors have attributed this band to highly oxidised species (like nitrates or nitrites)[66-68]. In addition, a strong band at 1085 cm^{-1} are likely to due to nitrates or nitrites too. K poison of VSZ catalyst has significant effects on the pattern of DRIFT spectra, presenting bands at 1410、1260、1085 cm^{-1}, and negative bands at 1200, 1140 cm^{-1}. Brønsted acid sites (1410 cm^{-1} [60, 64, 69]) and Lewis acid sites (1260 cm^{-1} [60-62]) still exit on the surface of KVSZ, however the strength of acidity decreased significantly compared with that of VSZ. A strong band at approximately 1085 cm^{-1} could be ascribed to bridged nitrates, which may be produced by highly oxidization of NH_3[70]. In addition, two negative bands at ca. 1140、1200 cm^{-1} were assigned to bidentate sulfates[71].

For CeVSZ(1) catalyst, both NH_3 coordinated on Lewis acid sites (1310 cm^{-1} [60-62]) and NH_4^+ species on Brønsted acid sites (1660、1435 cm^{-1} [60, 63, 64, 69]) were present after NH_3 adsorption. A small band appeared at 1355 cm^{-1}, belonging to highly oxidised species[66-68]. The addition of K has little effects on the DRIFT spectra of CeVSZ(1) catalyst (Fig. 10b), except that the band at 1355 cm^{-1} (due to highly oxidised species) became more distinguished.

Several results could be obtained from in situ DRIFT results: (a) VSZ catalyst has a strong acidity for adsorbing NH_3, however K would neutralize its acidity, resulting in a notable decrease of acidity, which should be the main reason for deactivation of KVSZ catalyst; (b) Considerable amount of acidity remains on the surface of KCeSZ and KCeVSZ(1), which is adequate for adsorption and activation of ammonia species.

4. Conclusion

A novel catalyst with dual resistance towards both alkali metals and SO_2 was developed in present work. vanadium and cerium supported on sulfated zirconia (Ce:V = 1:1) obtain the highest activity (> 97%) in the presence of K and SO_2, and no distinct decrease in NO conversion was observed in 400 min. CeO_2 supported on sulfated zirconia is an efficient catalyst with enhanced alkali resistance, however the formation of $Ce_2(SO_4)_3$ led to a permanent deactivation of catalyst. The partial replacement of Ce by V weakened SO_2 adsorption and oxidation, and led to the transformation of CeO_2 to $CeVO_4$, cutoffing of the reaction pathway from CeO_2 to $Ce_2(SO_4)_3$. In conclusion, vanadium and cerium supported on sulfated zirconia is an efficient catalyst for SCR with dual resistance to both alkali metals and SO_2 poisoning.

Acknowledgements

This work was financially supported by National Natural Science Foundation of China (NSFC-1278458), Changjiang Scholar Incentive Program (Ministry of Education, China,

2009), Zhejiang Provincial "151" Talents Program, Key Project of Zhejiang Provincial Science and Technology Program (No.2012C03003-3), Special Program for Social Development of Key Science and Technology Project of Zhejiang Province (2014C03025), and the Program for Zhejiang Leading Team of S&T Innovation (Grant No. 2013TD07) .

References

1. Z. Liu and S. Ihl Woo, *Catal. Rev.*, 2006, **48**, 43-89.
2. H. Wang, X. Chen, X. Weng, Y. Liu, S. Gao and Z. Wu, *Catal. Commun.*, 2011, **12**, 1042-1045.
3. L. Chen, J. H. Li and M. F. Ge, *Chem. Eng. J.*, 2011, **170**, 531-537.
4. D. Nicosia, I. Czekaj and O. Kröcher, *Appl. Catal. B*, 2008, **77**, 228-236.
5. Y. Peng, J. Li, W. Si, J. Luo, Y. Wang, J. Fu, X. Li, J. Crittenden and J. Hao, *Appl. Catal. B*, 2015, **168**, 195-202.
6. F. S. Tang, B. L. Xu, H. H. Shi, J. H. Qiu and Y. N. Fan, *Appl. Catal. B*, 2010, **94**, 71-76.
7. Y. Zheng, A. D. Jensen, J. E. Johnsson and J. R. Thøgersen, *Appl. Catal. B*, 2008, **83**, 186-194.
8. S. S. R. Putluru, S. B. Kristensen, J. Due-Hansen, A. Riisager and R. Fehrmann, *Catal. Today*, 2012, **184**, 192-196.
9. S. S. R. Putluru, S. Mossin, A. Riisager and R. Fehrmann, *Catal. Today*, 2011, **176**, 292-297.
10. S. S. R. Putluru, A. D. Jensen, A. Riisager and R. Fehrmann, *Catalysis Science & Technology*, 2011, **1**, 631-637.
11. Y. Peng, J. H. Li, L. Chen, J. H. Chen, J. Han, H. Zhang and W. Han, *Environ. Sci. Technol.*, 2012, **46**, 2864-2869.
12. B. Jiang, Z. Wu, Y. Liu, S. Lee and W. Ho, *J. Phys. Chem. C*, 2010, **114**, 4961-4965.
13. W. S. Kijlstra, M. Biervliet, E. K. Poels and A. Bliek, *Appl. Catal. B*, 1998, **16**, 327-337.
14. W. Xu, H. He and Y. Yu, *J. Phys. Chem. C*, 2009, **113**, 4426-4432.
15. C. Li, G. Zeng, Y. Zhou and X. Zhang, *Appl. Surf. Sci.*, 2015, **342**, 174-182.
16. Z. Liu, Y. Yi, J. Li, S. I. Woo, B. Wang, X. Cao and Z. Li, *Chem. Commun.* , 2013, **49**, 7726-7728.
17. H. Wang, S. Gao, F. Yu, Y. Liu, X. Weng and Z. Wu, *J. Phys. Chem. C*, 2015, **119**, 15077-15084.
18. S. Gao, P. Wang, X. Chen, H. Wang, Z. Wu, Y. Liu and X. Weng, *Catal. Commun.*, 2014, **43**, 223-226.
19. S. Gao, X. Chen, H. Wang, J. Mo, Z. Wu, Y. Liu and X. Weng, *J. Colloid Interf. Sci.*, 2013, **394**, 515-521.
20. I. S. Nam, J. W. Eldridge and J. Kittrell, *Ind. Eng. Chem. Res. Dev.*, 1986, **25**, 192-197.
21. M. J. Li, Z. H. Feng, G. Xiong, P. L. Ying, Q. Xin and C. Li, *J. Phys. Chem. B*, 2001, **105**, 8107-8111.
22. L. K. Noda, N. S. Gonçalves, S. M. de Borba and J. A. Silveira, *Vib. Spectrosc*, 2007, **44**, 101-107.
23. J. Matta, D. Courcot, E. Abi-Aad and A. Aboukais, *Chem. Mater.*, 2002, **14**, 4118-4125.
24. B. M. Reddy, A. Khan, Y. Yamada, T. Kobayashi, S. Loridant and J.-C. Volta, *J. Phys. Chem. B*, 2003, **107**, 5162-5167.
25. B. M. Reddy, P. M. Sreekanth, P. Lakshmanan and A. Khan, *J. Mol. Catal. A: Chem.*, 2006, **244**, 1-7.
26. J. Twu, C. J. Chuang, K. I. Chang, C. H. Yang and K. H. Chen, *Appl. Catal. B*, 1997, **12**, 309-324.
27. R. Flouty, E. Abi-Aad, S. Siffert and A. Aboukaïs, *J. Therm. Anal. Calorim.*, 2003, **73**, 727-734.
28. Y. Ying and Y. Rudong, *Thermochim. Acta* 1992, **202**, 301-306.
29. I. Giakoumelou, R. Caraba, V. Parvulescu and S. Boghosian, *Catal. Lett.* , 2002, **78**, 209-214.
30. C. Orsenigo, L. Lietti, E. Tronconi, P. Forzatti and F. Bregani, *Ind. Eng. Chem. Res.*, 1998, **37**, 2350-2359.
31. B.-W. Soh and I.-S. Nam, *Ind. Eng. Chem. Res.*, 2003, **42**, 2975-2986.
32. H. H. Phil, M. P. Reddy, P. A. Kumar, L. K. Ju and J. S. Hyo, *Appl. Catal. B*, 2008, **78**, 301-308.
33. M. Kobayashi, R. Kuma, S. Masaki and N. Sugishima, *Appl. Catal. B*, 2005, **60**, 173-179.
34. G. Y. Xie, Z. Y. Liu, Z. P. Zhu, Q. Y. Liu, J. Ge and Z. G. Huang, *J. Catal.*, 2004, **224**, 36-41.
35. C. L. Bianchi, S. Ardizzone and G. Cappelletti, *Surf. Interface Anal.*, 2004, **36**, 745-748.
36. S. Ardizzone, C. L. Bianchi and M. Signoretto, *Appl. Surf. Sci.*, 1998, **136**, 213-220.
37. L. Kumari, W. Z. Li, J. M. Xu, R. M. Leblanc, D. Z. Wang, Y. Li, H. Guo and J. Zhang, *Cryst. Growth. Des.*, 2009, **9**, 3874-3880.
38. X. Chen, H. Wang, S. Gao and Z. Wu, *J. Colloid Interf. Sci.*, 2012, **377**, 131-136.
39. V. Matolín, I. Matolínová, F. Dvořák, V. Johánek, J. Mysliveček, K. C. Prince, T. Skála, O. Stetsovych, N. Tsud, M. Václavů and B. Šmíd, *Catal. Today*, 2012, **181**, 124-132.
40. D. R. Milburn, R. A. Keogh, R. Srinivasan and B. H. Davis, *Appl. Catal. A*, 1996, **147**, 109-125.
41. M. Y. Smirnov, A. Kalinkin, A. Pashis, A. Sorokin, A. Noskov, V. Bukhtiyarov, K. Kharas and M. Rodkin, *Kinet. Catal.*, 2003, **44**, 575-583.
42. M. Y. Smirnov, A. V. Kalinkin, A. V. Pashis, A. M. Sorokin, A. S. Noskov, K. C. Kharas and V. I. Bukhtiyarov, *J. Phys. Chem. B*, 2005, **109**, 11712-11719.
43. Y. Peng, C. Wang and J. Li, *Appl. Catal. B*, 2014, **144**, 538-546.
44. Y. Yang, S. P. Albu, D. Kim and P. Schmuki, *Angew. Chem.*, 2011, **123**, 9237-9241.
45. J. Bao, M. Zhou, Y. Zeng, L. Bai, X. Zhang, K. Xu and Y. Xie, *J. Mater. Chem. A*, 2013, **1**, 5423-5429.
46. H.-L. Koh and H.-K. Park, *J. Ind. Eng. Chem.* , 2013, **19**, 73-79.
47. J. Wu and Y.-T. Cheng, *J. Catal.*, 2006, **237**, 393-404.
48. F. Loeker, P. C. Marr and S. M. Howdle, *Colloids Surf., A* 2003, **214**, 143-150.
49. B. Anderson, Z. Dang and B. Morrow, *J. Phys. Chem.*, 1995, **99**, 14444-14449.
50. J. P. Dunn, J.-M. Jehng, D. S. Kim, L. E. Briand, H. G. Stenger and I. E. Wachs, *J. Phys. Chem. B*, 1998, **102**, 6212-6218.
51. Q. Ma, Y. Liu and H. He, *J. Phys. Chem. A*, 2008, **112**, 6630-6635.
52. A. Goodman, P. Li, C. Usher and V. Grassian, *J. Phys. Chem. A*, 2001, **105**, 6109-6120.

53. M. M. Thompson and R. A. Palmer, *Appl. Spectrosc.*, 1988, **42**, 945-951.
54. S. J. Hug and D. Bahnemann, *J. Electron. Spectrosc. Relat. Phenom.* , 2006, **150**, 208-219.
55. J. Degenhardt and A. J. McQuillan, *Chem. Phys. Lett.* , 1999, **311**, 179-184.
56. P. A. Bhatt and P. Paul, *J. Chem. Sci.* , 2008, **120**, 267-273.
57. P. Z. Araujo, C. B. Mendive, L. A. G. Rodenas, P. J. Morando, A. E. Regazzoni, M. A. Blesa and D. Bahnemann, *Colloids Surf., A* 2005, **265**, 73-80.
58. S. S. R. Putluru, A. D. Jensen, A. Riisager and R. Fehrmann, *Catal. Commun.*, 2012, **18**, 41-46.
59. S. S. R. Putluru, A. Riisager and R. Fehrmann, *Appl. Catal. B*, 2011, **101**, 183-188.
60. S. D. Lin, A. C. Gluhoi and B. E. Nieuwenhuys, *Catal. Today*, 2004, **90**, 3-14.
61. L. Castoldi, R. Bonzi, L. Lietti, P. Forzatti, S. Morandi, G. Ghiotti and S. Dzwigaj, *J. Catal.*, 2011, **282**, 128-144.
62. M. A. Larrubia, G. Ramis and G. Busca, *Appl. Catal. B*, 2000, **27**, L145-L151.
63. L. Chen, J. Li and M. Ge, *Environ. Sci. Technol.*, 2010, **44**, 9590-9596.
64. X. Wu, W. Yu, Z. Si and D. Weng, *Front. Env. Sci. Eng.*, 2013, **7**, 420-427.
65. Y. Yu, J. Wang, J. Chen, X. Meng, Y. Chen and C. He, *Ind. Eng. Chem. Res.*, 2014, **53**, 16229-16234.
66. G. Ramis and M. Angeles Larrubia, *J. Mol. Catal. A: Chem.*, 2004, **215**, 161-167.
67. M. A. Larrubia, G. Ramis and G. Busca, *Appl. Catal. B*, 2001, **30**, 101-110.
68. G. Qi and R. T. Yang, *J. Phys. Chem. B*, 2004, **108**, 15738-15747.
69. H. Schneider, S. Tschudin, M. Schneider, A. Wokaun and A. Baiker, *J. Catal.*, 1994, **147**, 5-14.
70. M. Kantcheva and E. Z. Ciftlikli, *J. Phys. Chem. B*, 2002, **106**, 3941-3949.
71. S. Koyande, R. Jaiswal and R. Jayaram, *Ind. Eng. Chem. Res.*, 1998, **37**, 908-913.

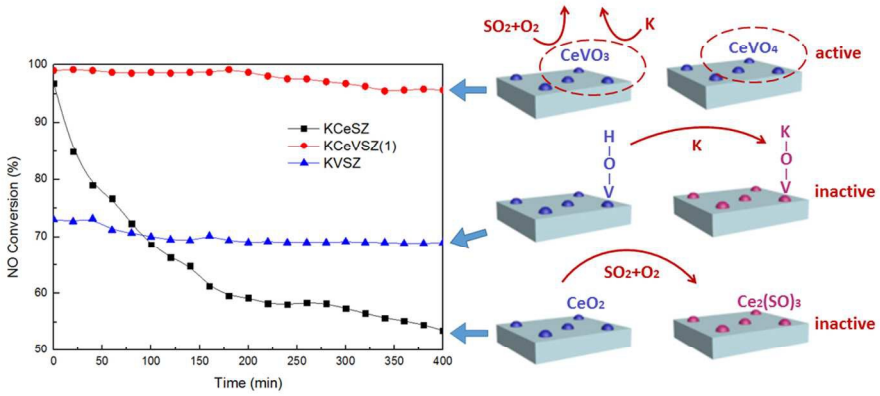

338x169mm (96 x 96 DPI)